



Materials and Energy Research Center

MERC

Contents lists available at [ACERP](#)

Advanced Ceramics Progress

Journal Homepage: www.acerp.ir

Advanced Ceramics Progress

Original Research Article

Enhancing the Electrical Properties of Bismuth Titanate Ceramics Using Zinc Oxide Nanoparticles as Sintering Aid

Fatemeh Alidoosti shahraki ^a, Hajar Ahmadimoghadam ^b*^a MSc, Department of Materials Engineering, Faculty of Engineering, University of Shahrekord, Shahrekord, Iran.^b Associate Professor, Department of Materials Engineering, Faculty of Engineering, University of Shahrekord, Shahrekord, Iran.* Corresponding Author Email: hajar.ahmadi@sku.ac.ir (H. Ahmadimoghadam)URL: https://www.acerp.ir/article_205719.html

ARTICLE INFO

Article History:

Received: 10 May 2024

Revised: 31 May 2024

Accepted: 7 September 2024

Keywords:

Bismuth Titanate,
Zinc Oxide Nanoparticles,
Sintering,
Dielectric Properties,
Microstructure

ABSTRACT

In this study, bismuth titanate (BIT) powder was synthesized through solid-state synthesis method. Then, the effect of zinc oxide (ZnO) nanoparticles as a sintering aid on the electrical properties of BIT ceramic was investigated. The weight percentages of ZnO used in this study were 0.3, 0.6, and 1.2. Disc-shaped samples were prepared using the uniaxial pressing method and sintered at the temperatures of 1025, 1075, and 1125 °C for 1, 2, and 5 h at the heating rates of 3, 5, and 10 °C/min. The highest density values were achieved under the optimal sintering conditions of 1075 °C, 2 h, and a heating rate of 5 °C/min. Addition of ZnO nanoparticles improved the densification of the BIT ceramics. In the sample containing 1.2 wt.% of ZnO, a secondary phase of Zn₂TiO₄ was identified. Incorporation of ZnO nanoparticles resulted in an increase in the dielectric constant, a reduction in dielectric loss, and improvement in the piezoelectric and ferroelectric properties of the BIT ceramics. These enhancements contributed to increased density and reduced electrical conductivity. The best results were obtained with the sample containing 0.6 wt.% of nano ZnO characterized by a high dielectric constant (312), low dielectric loss (tanδ = 0.01), high piezoelectric coefficient (d₃₃ = 21 pC/N), and high remnant polarization (4.25 μC/cm²).

<https://doi.org/10.30501/acp.2024.456603.1152>

1. INTRODUCTION

Layered ferroelectric bismuth-containing structures (BLSFs) have received significant attention over the past two decades owing to their outstanding electrical properties as lead-free piezoelectric materials at high temperatures. They also allow for customized properties by adjusting the chemical composition and number of layers. BLSF ceramics, with their high Curie temperature (T_C), fatigue resistance, and thermal stability, can be used at temperatures above 400 °C. The general formula for BLSFs is (Bi₂O₂)²⁺(A_{n-1}B_nO_{3n+3})²⁻, which consists of perovskite-like layers (A_{n-1}B_nO_{3n+3})²⁻ separated by (Bi₂O₂)²⁺ layers along the crystallographic c-axis. In this formula, n (1 ≤ n ≤ 5) denotes the number of perovskite

layers. BLSF crystal structures have a large c/a ratio based on the value of n (c/a ≈ 1.5(n+1)), thus resulting in the formation of plate-like grains with a high aspect ratio and significant anisotropy in their electrical properties [1-3]. It has been reported that achieving highly oriented and textured grains through techniques such as applying pressure during the solid-state sintering process and directionally controlled grain growth would lead to improved electrical properties [1,4].

Among the BLSF family, bismuth titanate (Bi₄Ti₃O₁₂, n=3, BIT) has received significant attention due to its high curie temperature (approximately 670 °C), strong inherent polarization, and notable fatigue resistance. BIT ceramics, as a suitable choice for high-temperature

Please cite this article as: Alidoosti shahraki, F. & Ahmadimoghadam, H. (2023). "Enhancing the Electrical Properties of Bismuth Titanate Ceramics Using Zinc Oxide Nanoparticles as Sintering Aid" *Advanced Ceramics Progress*, Vol. 9, No. 3, (2023), 50-56. <https://doi.org/10.30501/acp.2024.456603.1152>

2423-7485/© 2023 The Author(s). Published by MERC.

This is an open access article under the CC BY license (<https://creativecommons.org/licenses/by/4.0/>).

piezoelectric applications, demonstrate excellent performance in non-volatile random-access memories (NvRAMs) [2]. However, BIT ceramics have some drawbacks including their relatively low piezoelectric coefficient (d_{33} less than 10 pC/N) due to the challenge of achieving easy polarization caused by its high leakage current. Additionally, the high dielectric loss ($\tan \delta$) and low electrical resistivity at elevated temperatures, attributed to oxygen vacancies resulting from bismuth volatilization during the sintering process, can limit the potential applications of BIT ceramics [1,5].

In recent years, several technologies have been introduced to overcome the limitations of BIT ceramics, thereby improving their properties. Some of these solutions include hot pressing, spark plasma sintering, directional grain growth, and use of dopants and additives [4, 6-8]. Among these methods, application of dopants and additives is more accessible and practical since it can significantly modify the sintering process, microstructure, and electrical properties of BIT ceramics [9,10]. Studies have shown that substituting cations in the B position greatly enhanced the piezoelectric properties of BLSFs [2,5,11]. Moreover, substituting V^{5+} cations for Ti^{4+} through the reduction of oxygen and bismuth vacancies led to reduced current leakage, easier domain movement, and increased polarization, thereby improving the ferroelectric and dielectric properties of BIT ceramics [12]. The introduction of Fe^{3+} ions into the Ti^{4+} position of the BIT structure has proved to enhance its ferroelectric properties and ferromagnetism [13]. Similarly, simultaneous use of Nb^{5+} and Fe^{3+} cations in the B position of the BIT structure results in a decrease in the dielectric constant and induction of ferromagnetism [2]. Additionally, W/Cr co-doped $Bi_4Ti_3O_{12}$ ceramics exhibited an improvement in their piezoelectric coefficient and an increase in their electrical resistance due to the lattice distortion [14]. It was reported that addition of zinc oxide to bismuth potassium titanate ($(Bi_{0.5}K_{0.5})TiO_3$) ceramic resulted in grain growth and increased density. When added in amounts less than 2 wt%, it improved the dielectric constant and piezoelectric coefficient. These improvements were attributed to the formation of oxygen vacancies and distortion of the crystal lattice [15]. The simultaneous use of W/Zn dopants has resulted in an increase in the electrical conductivity and a decrease in the dielectric constant of bismuth titanate ceramic [16]. Research has demonstrated that the incorporation of zinc oxide has the potential to enhance the piezoelectric and dielectric properties of various ceramics, including sodium potassium niobates and barium titanates [17,18].

Although a great deal of research has been conducted on the effect of different cations as dopants on the electrical properties of BIT ceramics, there is limited research on additives as sintering aids. In this respect, the main objective of this study was to investigate the effect of zinc oxide nanoparticles (ZnO) as a sintering aid on

the properties of BIT ceramics. BIT powder was synthesized using the solid-state method, and varying amounts (0.3, 0.6, and 1.2 wt.%) of ZnO nanoparticles were added. The current study also examined the impact of nano ZnO additive on the microstructure and dielectric properties of BIT ceramics.

2. MATERIALS AND METHODS

Bismuth oxide (Bi_2O_3) and titanium oxide (TiO_2) with the purity of 99.9% were used for the synthesis of bismuth titanate powder (BIT) with the chemical formula of $Bi_4Ti_3O_{12}$. The raw materials were accurately weighed according to the BIT stoichiometry and then mixed in a planetary mill with zirconia balls in ethanol at a speed of 250 rpm for 5 hours. Subsequently, the resulting powder was calcined at 850 °C for 3 hours. Zinc oxide nanoparticles (99.9%, ≤ 70 nm, Advanced Materials US) were added to the synthesized BIT powder in weight percentages of 0.3, 0.6, and 1.2. A planetary mill operating at 300 rpm for 5 hours ensured a uniform mixture of BIT powder and nano zinc oxide. Disc-shaped samples were fabricated using the uniaxial pressing method at the pressure of 200 MPa with the diameter of 1 cm and thickness of approximately 2 mm. The samples were labeled as follows: BIT (sample without additive), BIT-0.3 Zn (sample with 0.3 wt.% nano ZnO), BIT-0.6 Zn (sample with 0.6 wt.% nano ZnO), and BIT-1.2 Zn (sample with 1.2 wt.% nano ZnO). In order to determine the optimal sintering conditions, the samples were heated at the temperatures of 1025, 1075, and 1125 °C for 1, 2, and 5 hours at the heating rates of 3, 5, and 10 °C/min.

The density of the samples was determined using the Archimedes immersion method following the ASTM C20-87 standard. In this experiment, X-Ray Diffraction (XRD) (Asenware model AW-XDM 300, Cu- α radiation with a wavelength of 1.5418 Å) and Scanning Electron Microscopy (FE-SEM, model 450 FEG, FEI QUANTA) were employed to examine the phase and microstructure of the samples, respectively. Dielectric properties, including dielectric constant and dielectric loss ($\tan \delta$), were measured using an LCR-meter model OCT1010 at room temperature within the frequency range of 100 Hz to 100 kHz. The sample surfaces were initially coated with silver paste using a brush and then heated at 400 °C for ten minutes. A piezometer (Berlincourt quasistaticmeter model) was used to measure the piezoelectric coefficient at room temperature and frequency of 100 Hz. The polarization versus electric field (P-E) ferroelectric hysteresis loops were recorded at a frequency of 50 Hz at room temperature using a Sawyer-Tower circuit.

3. RESULTS AND DISCUSSION

Variations in the density of the samples, expressed as the weight percentage of nano ZnO, at different sintering temperatures are shown in Figure 1. The sintering time was 2 hours, and the heating rate was 5 °C/min. As shown

in Figure 1, use of nano ZnO additive has notably improved the density of BIT ceramics. The density of BIT ceramic increases as the amount of nano ZnO increases. Previous studies have stated that ZnO in bismuth titanate-based ceramics enhances densification by creating a liquid phase during the sintering process. This liquid phase, which contains a high concentration of bismuth oxide, forms in a small amount during sintering through the reaction between bismuth oxide and ZnO at the eutectic temperature of approximately 750 °C [16,19]. According to Equation 1, replacement of Zn^{2+} ions results in the creation of oxygen vacancies ($V_{O^{**}}$), which facilitates atomic diffusion during sintering and improves densification [20]. The BIT-0.6 Zn and BIT-1.2 Zn samples share quite similar density values. The highest density values were achieved when the samples were sintered at the temperature of 1075 °C. Therefore, the optimal sintering temperature can be considered as 1075 °C. The densification of ceramics during sintering occurs through the mechanism of atomic diffusion, and temperature is the main parameter that affects the diffusion of atoms [20]. Therefore, the low densities of the samples sintered at 1025 °C may be attributed to the insufficient atoms diffusion. According to the results, the density of the samples sintered at the temperature of 1125 °C is lower than that of samples sintered at 1075 °C, which can be attributed to the increased volatility of bismuth oxide at higher temperatures [21]. Based on Figure 1, the density of BIT ceramics is highly dependent on the sintering temperature. At temperatures lower than the optimum temperature, density significantly decrease due to insufficient diffusion while at temperatures higher than the optimum temperature, it happens due to the increased volatility of bismuth oxide.

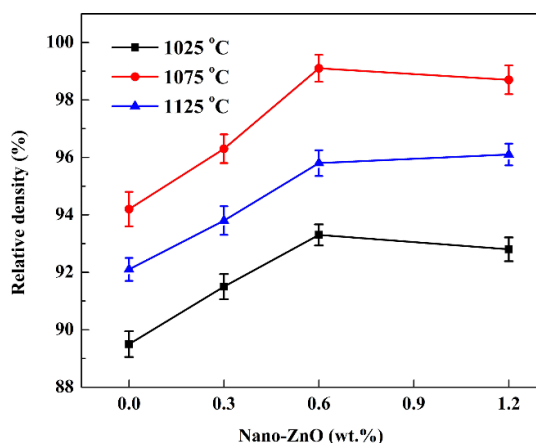


Figure 1. Variations in density of samples as a function of ZnO amount at different sintering temperatures.

Figure 2 illustrates the changes in the sample density, represented as weight percentage of nano ZnO, at different storage times during sintering. The samples were sintered at an optimal temperature of 1075 °C for various durations at the heating rate of 5 °C/min. According to the obtained results, the duration of maintaining the samples at the sintering temperature has a significant effect on the density of BIT ceramics. The optimal duration is determined to be 2 hours, as increasing the sintering time from 1 to 2 hours leads to an increase in sample density. However, if the duration is extended to 5 hours, a significant decrease would be observed in the sample density, even lower than the samples sintered for only 1 hour. This decrease in the density during the extended sintering times can be attributed to the increased volatility of bismuth oxide.

The density variations of the samples at different heating rates, in terms of the amount of nano ZnO, are shown in Figure 3. These samples were sintered at different heating rates at the optimal temperature of 1075 °C for 2 hours. According to the results, the heating rate significantly affects the density of the BIT ceramic. The optimal heating rate, as indicated in Figure 3, is 5 °C/min, hence the highest density for the samples. The samples sintered at a lower heating rate of 3 °C/min had a lower density. At lower heating rates, coarsening and excessive grain growth dominate during sintering. In this case, not only the porosity remains in the body but also its size increases, hence a decrease in density [20]. The reduction in density at high heating rates (10 °C/min) can be attributed to the internal stresses caused by the significant difference in the growth rates perpendicular and parallel to the plane of the layered BLSF structures. This substantial difference in the growth rates at high heating rates can generate internal stresses and microcracks, ultimately resulting in density reduction [21].

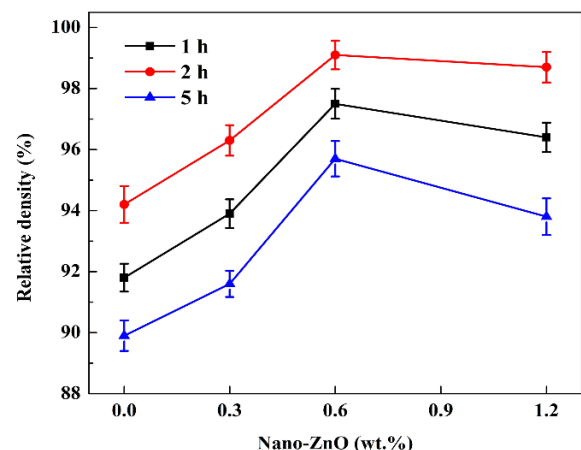


Figure 2. Variations in density of samples as a function of ZnO amount with different sintering times.

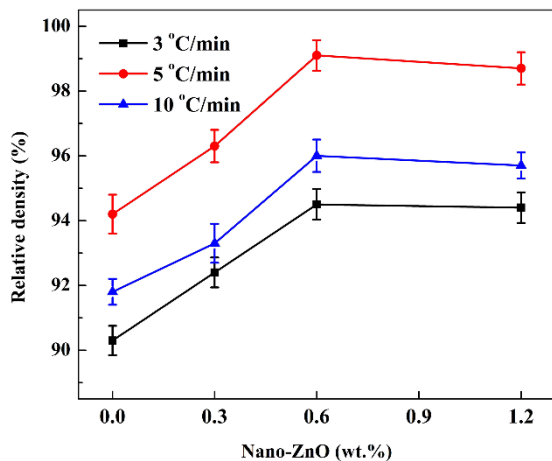


Figure 3. Variations in sample density as a function of the amount of ZnO with different heating rates

Figure 4 shows the XRD patterns of the samples sintered under optimized conditions with different weight percentages of ZnO. The identified diffraction peaks in the patterns correspond to the $\text{Bi}_4\text{Ti}_3\text{O}_{12}$ phase with an orthorhombic structure (JCPDS No. 96-591-0229). No secondary phases or impurities are observed in the BIT-0.3 Zn and BIT-0.6 Zn samples. A comparison of the ionic radii of Zn^{2+} (0.74 Å), Ti^{4+} (0.605 Å), and Bi^{3+} (1.03 Å) shows that the possibility of substituting Zn^{2+} ions in the B-site of the perovskite layer of BIT instead of Ti^{4+} ions is higher than other ones. Zn^{2+} ions are smaller than Bi^{3+} ions for occupying the A-site [16, 19]. Therefore, there is a possibility of Zn^{2+} ions entering the crystal lattice of BIT and forming a solid solution. In the BIT-1.2 Zn sample, in addition to the peaks corresponding to the $\text{Bi}_4\text{Ti}_3\text{O}_{12}$ phase, three other peaks with low intensity are detected. These peaks correspond to the Zn_2TiO_4 phase with a cubic structure (JCPDS No. 96-900-1693). This phase has been reported in zinc-doped bismuth titanate compounds [15,16,19]. Of note, the solubility limit of Zn in the base BIT ceramics is less than 1 wt% [15,16]. The XRD patterns indicate that addition of ZnO has a significant effect on the peak intensities, hence a decrease in the intensity of the (117) peak and an increase in the intensities of the (006), (008), and (0014) peaks as the amount of added ZnO increases. This can indicate changes in the microstructure and grain orientation of the BIT ceramic in the presence of ZnO additives [16].

The SEM images of the fractured surfaces of both BIT and BIT-0.6 Zn samples are illustrated in Figure 5. Clearly, addition of ZnO has a significant effect on the microstructure of the BIT ceramic. The BIT-0.6 Zn sample is characterized by a dense microstructure, and the BIT sample by porosities. The grain morphology is characterized by plate-like and layered structures, with a noticeable difference in grain orientation between the BIT-0.6 Zn and BIT samples. Previous studies have demonstrated that additives in the BIT ceramics can

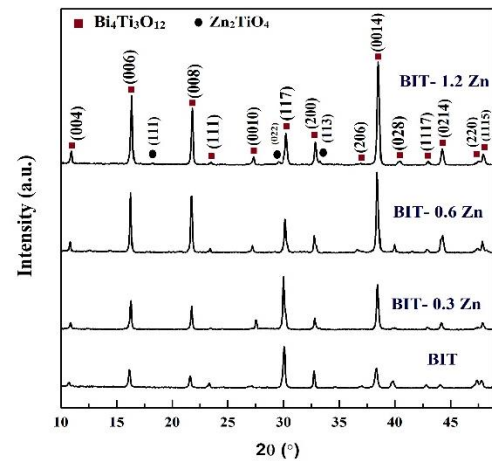


Figure 4. XRD patterns of sintered samples

induce preferential grain growth and grain orientation [1,4,9].

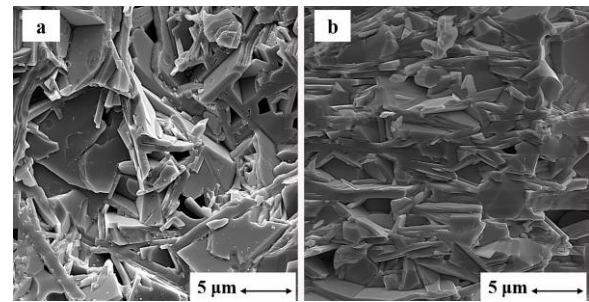


Figure 5. SEM images of fracture surfaces of samples: (a) BIT and (b) BIT -0.6 Zn

Figure 6 illustrates the variations in the dielectric constant of the samples, which were measured at room temperature in the frequency range of 100 Hz to 100 kHz. The results indicate that addition of nano ZnO increases the dielectric constant of the BIT ceramic. The highest dielectric constant values were obtained in the BIT-0.6 Zn sample. Additionally, the dependence of the dielectric constant on the frequency in the samples with ZnO additive is lower than that in the pure BIT sample. The improvement in the dielectric constant in the presence of nano ZnO additive can be attributed to higher density and lower porosity in these samples [22]. Several studies have also indicated that changes in the grain growth direction can enhance the dielectric properties [16]. Given the difference in the ionic radii between Zn^{2+} (0.74 Å) and Ti^{4+} ions (0.605 Å), substitution of Zn^{2+} ions at the B site can cause lattice distortion and local deformation of the unit cell. Preethi et. al. reported that lattice distortion resulting from the substitution of solute atoms with different radii in the structure increased the dielectric constant [23]. In addition, the decrease in the dielectric constant values of the BIT-1.2 Zn sample could

be attributed to the presence of the secondary phase Zn_2TiO_4 in this sample. They also remarked that the Zn_2TiO_4 phase had a very low dielectric constant [19].

Figure 7 shows the variations in the dielectric loss of the sample, measured at room temperature in the frequency range of 100 Hz to 100 kHz. The results indicate that incorporation of ZnO reduces the dielectric loss of the BIT ceramic. The BIT-0.6 sample had the lowest dielectric loss values and followed by addition of ZnO, the dielectric loss values in the BIT -1.2 Zn sample increased, compared to the other two samples. However, the dielectric loss values in the BIT -1.2 Zn sample remained lower than those of the pure BIT ceramic. The increase in the dielectric loss of the BIT-1.2 Zn sample can be attributed to the presence of the Zn_2TiO_4 impurity phase.

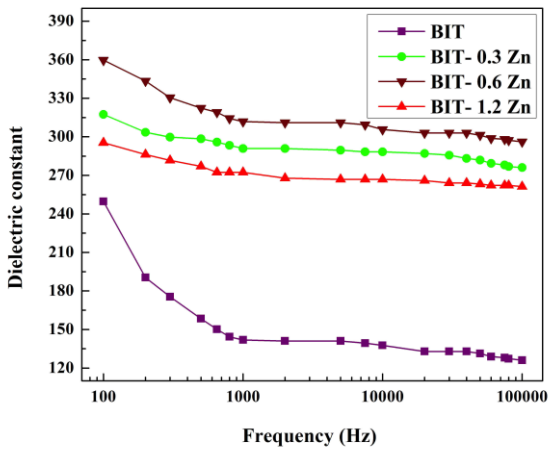


Figure 6. Frequency dependence of dielectric constant for samples measured at room temperature

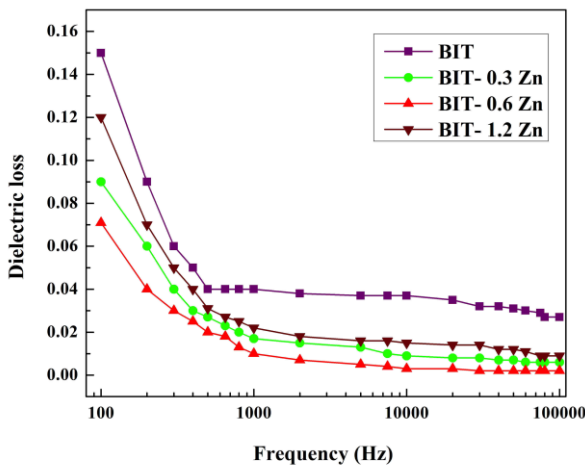


Figure 7. Frequency dependence of dielectric loss for samples measured at room temperature

Figure 8 shows the dielectric constant and dielectric loss of the samples, measured at the frequency of 1 kHz, as a function of the amount of ZnO. The results indicate a significant improvement in the dielectric properties of

the BIT ceramic when using ZnO additive. Among the samples, the BIT -0.6 Zn sample demonstrates the highest dielectric constant and the lowest dielectric loss. Notably, the dielectric constant value for the BIT -0.6 Zn sample is 312, while for the BIT sample, it is 142. The dielectric loss value for the BIT sample was reduced from 0.04 to 0.01 in the BIT -0.6 Zn sample. The enhancement in the dielectric properties in the presence of ZnO nanoparticles can be attributed to higher density, lattice distortion in the crystal structure, and grain orientation [4,5].

The ac conductivity (σ_{ac}) of the dielectric materials is calculated using Equation 2 where ϵ_0 represents the permittivity of vacuum, ϵ' the permittivity of the material, $\tan\delta$ the dielectric loss, and ω ($2\pi f$) the angular frequency of the applied ac field [24]. The graph of the ac conductivity calculated from Equation 2 for the samples as a function of frequency is shown in Figure 9.

$$\sigma_{ac} = \epsilon_0 \epsilon' \omega \tan\delta \tag{2}$$

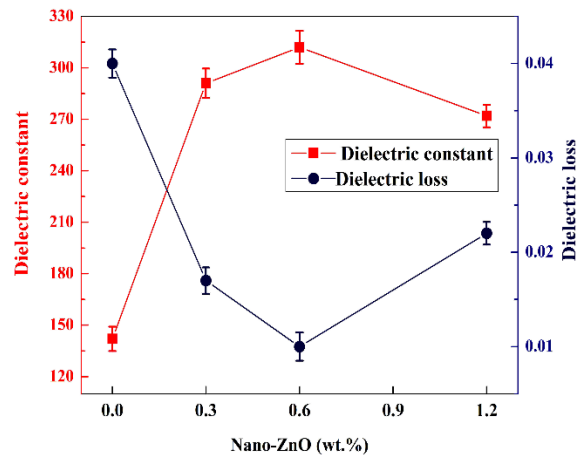


Figure 8. Dielectric constant and dielectric loss of samples as a function of ZnO amount measured at 1 kHz

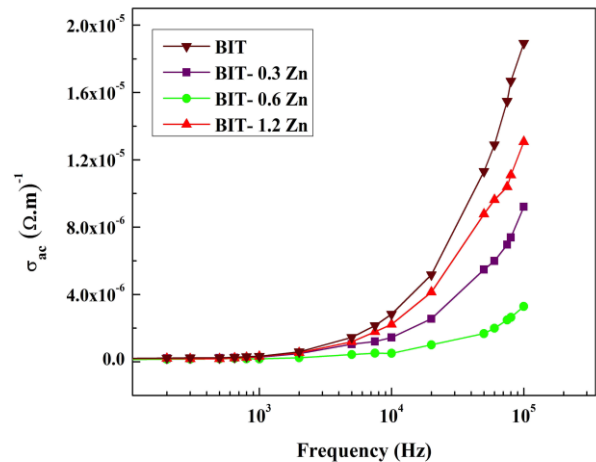


Figure 9. Frequency dependence of the ac conductivity for samples

The ac conductivity values for all samples remain constant at low frequencies and represent the dc conductivity of the dielectric material. The ac conductivity increases as the applied field frequency increases. Beyond a certain frequency known as the hopping frequency (occurring at around 10^4 Hz for the samples), there is a significant increase in the ac conductivity, indicating the presence of a frequency hopping region. This behavior can be justified by the Maxwell-Wagner surface model according to which, charge carriers become trapped at grain boundaries, structural defects, and imperfections within the material, impeding their free movement. As the frequency increases, the charge carriers gain sufficient energy to overcome these barriers, resulting in a substantial increase in ac conductivity [10,24]. According to Figure 9, addition of ZnO nanoparticles leads to a decrease in the ac conductivity of the BIT ceramic. The BIT-0.6 Zn sample had the lowest ac conductivity values. According to Equation 2, the ac conductivity is determined by the permittivity and dielectric loss of the samples. Followed by addition of ZnO nanoparticles, the permittivity increases while the dielectric loss decreases, resulting in a reduction in ac conductivity. Therefore, the impact of ZnO nanoparticles on reducing the dielectric loss is more significant than the increase in the permittivity, hence a decrease in ac conductivity. This decrease, which is indicative of an increase in the electrical resistance, can contribute to the enhancement of dielectric properties.

Figure 10 represents the variations in the piezoelectric coefficient (d_{33}) for the samples as a function of the amount of zinc oxide nanoparticles. A significant limitation of BIT ceramics is their low piezoelectric coefficient. According to the obtained results, addition of zinc oxide nanoparticles improves the piezoelectric coefficient of the BIT ceramic. Figure 11 shows the polarization hysteresis loop for the BIT and BIT -0.6 Zn samples. It also indicates that the saturation and remnant polarization values for the BIT -0.6Zn sample are $12 \mu\text{C}/\text{cm}^2$ and $4.25 \mu\text{C}/\text{cm}^2$, respectively while for the BIT sample, they are $8.5 \mu\text{C}/\text{cm}^2$ and $2.32 \mu\text{C}/\text{cm}^2$, respectively. The coercive field value for both samples is obtained as approximately 14 kV/cm. According to Equation 1, substituting Zn^{2+} ions at the B site creates oxygen vacancies which, along with Zn^{2+} ions, induce local distortions in the perovskite unit cells. Additionally, the electric dipoles from $\text{Zn}_{\text{Ti}}-\text{V}_{\text{O}}^{\bullet\bullet}$ defects and elastic dipoles from the disorder of the unit cell caused by oxygen vacancies are formed. These dipoles have good excitation capabilities that contribute to the improvement in the dielectric properties. Further, the disorder of the unit cell facilitates the alignment of ferroelectric domains during polarization, resulting in improved piezoelectric and ferroelectric properties [15, 16].

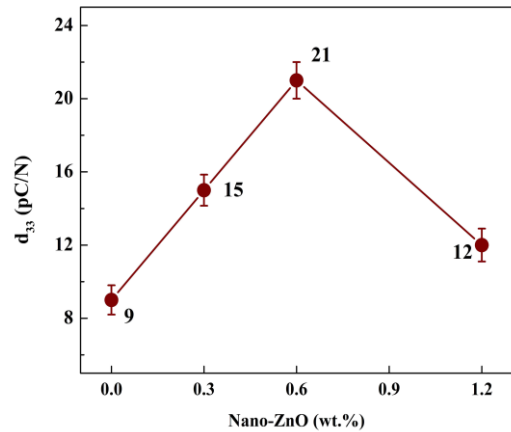


Figure 10. Piezoelectric coefficient of samples as a function of the amount of ZnO

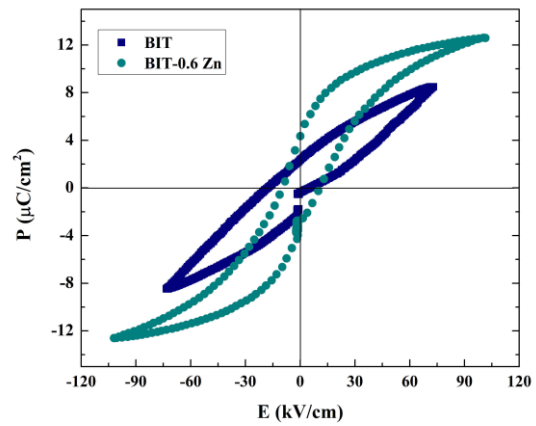


Figure 11. Polarization hysteresis loop for BIT and BIT -0.6 Zn samples

4. CONCLUSIONS

This study investigated the impact of zinc oxide nanoparticles as the sintering aid (at concentrations of 0.3, 0.6, and 1.2 wt %) on different properties of bismuth titanate ceramic. The findings of this study were summarized as follows:

1. To achieve high-density samples, the optimal sintering conditions required were determined as the temperature of 1075°C , holding time of 2 hours, and heating rate of $5^\circ\text{C}/\text{min}$.
2. Incorporation of ZnO nanoparticle sintering aid enhanced the densification of the BIT ceramic.
3. Addition of 1.2 wt% ZnO resulted in the formation of a secondary phase (Zn_2TiO_4) in the BIT ceramic.
4. The ZnO sintering aid additive modified the grain growth orientation in the microstructure of the BIT ceramic.
5. The ZnO sintering aid significantly increased the dielectric constant and decreased the dielectric loss of the BIT ceramic. The sample with 0.6 wt% ZnO exhibited a maximum dielectric constant of 312,

which was approximately twice that of the pure BIT sample at the frequency of 1 kHz.

6. A high piezoelectric coefficient of 21 pC/N was observed in the sample with 0.6 wt% ZnO, which was more than twice that of the pure BIT sample.
7. The remnant polarization value of the sample with 0.6 wt% ZnO, $4.2 \mu\text{C}/\text{cm}^2$, was approximately 82% higher than that of the pure BIT sample.

REFERENCES

1. Jiang, D., Zhou, Z., Liang, R., Dong, X., "Highly orientated $\text{Bi}_4\text{Ti}_3\text{O}_{12}$ piezoceramics prepared by pressureless sintering", *Journal of the European Ceramic Society*, Vol. 41(2), (2021),1244-1250. <https://doi.org/10.1016/j.jeurceramsoc.2020.09.039>
2. Lavado, C., Stachiotti, M. G., "Fe³⁺/Nb⁵⁺ co-doping effects on the properties of Aurivillius $\text{Bi}_4\text{Ti}_3\text{O}_{12}$ ceramics", *Journal of Alloys and Compounds*, Vol.731, (2018),914-919. <https://doi.org/10.1016/j.jallcom.2017.10.112>
3. Badge, S. K., Deshpande, A. V., "Study of dielectric and ferroelectric properties of Bismuth Titanate ($\text{Bi}_4\text{Ti}_3\text{O}_{12}$) ceramic prepared by sol-gel synthesis and solid state reaction method with varying sintering temperature", *Solid State Ionics*, Vol. 334, (2019), 21-28. <https://doi.org/10.1016/j.ssi.2019.01.028>
4. Hong, S. H., Trolrier-McKinstry, S., Messing, G. L., "Dielectric and electromechanical properties of textured niobium-doped bismuth titanate ceramics", *Journal of the American Ceramic Society*, Vol. 83(1), (2000), 113-118. <https://doi.org/10.1111/j.1151-2916.2000.tb01157.x>
5. Xie, X., Zhou, Z., Liang, R., Dong, X., "Significantly enhanced piezoelectric performance in $\text{Bi}_4\text{Ti}_3\text{O}_{12}$ -based high-temperature piezoceramics via oxygen vacancy defects tailoring", *Journal of Materiomics*, Vol. 7(1), (2021),59-68. <https://doi.org/10.1016/j.jimat.2020.08.003>
6. Liu, J., Shen, Z., Yan, H., Reece, M. J., Kan, Y., Wang, P., "Dielectric, piezoelectric, and ferroelectric properties of grain-orientated $\text{Bi}_{3.25}\text{La}_{0.75}\text{Ti}_3\text{O}_{12}$ ceramics", *Journal of applied physics*, Vol. 102(10), (2007), 104107. <https://doi.org/10.1063/1.2812697>
7. Zhang, H., Yan, H., Zhang, X., Reece, M.J., Liu, J., Shen, Z., Kan, Y. Wang, P., "The effect of texture on the properties of $\text{Bi}_{3.15}\text{Nd}_{0.85}\text{Ti}_3\text{O}_{12}$ ceramics prepared by spark plasma sintering", *Materials Science and Engineering:A*, Vol. 475, (2008), 92-95. <https://doi.org/10.1016/j.msea.2006.12.144>
8. Zhang, H., Ke, H., Luo, H., Guo, P., Yang, B., Jia, D., Zhou, Y., "Effects of spark plasma sintering on ferroelectricity of $0.8\text{Bi}_{3.15}\text{Nd}_{0.85}\text{Ti}_3\text{O}_{12}-0.2\text{CoFe}_2\text{O}_4$ composite ceramic", *Journal of the European Ceramic Society*, Vol. 38(5), (2018), 2353-2359. <https://doi.org/10.1016/j.jeurceramsoc.2018.01.011>
9. Bokolia, R., Thakur, O. P., Rai, V. K., Sharma, S. K., Sreenivas, K. J. C. I., "Dielectric, ferroelectric and photoluminescence properties of Er³⁺ doped $\text{Bi}_4\text{Ti}_3\text{O}_{12}$ ferroelectric ceramics", *Ceramics International*, Vol. 41(4), (2015),6055-6066. <https://doi.org/10.1016/j.ceramint.2015.01.062>
10. Subohi, O., Bowen, C. R., Malik, M. M., Kurchania, R., "Dielectric spectroscopy and ferroelectric properties of magnesium modified bismuth titanate ceramics", *Journal of Alloys and Compounds*, Vol. 688, (2016), 27-36. <https://doi.org/10.1016/j.jallcom.2016.07.173>
11. Hou, J., Kumar, R. V., Qu, Y., Krsmanovic, D., "B-site doping effect on electrical properties of $\text{Bi}_4\text{Ti}_{3-2x}\text{Nb}_x\text{Ta}_x\text{O}_{12}$ ceramics", *Scripta Materialia*, Vol. 61, (2009),664-667. <https://doi.org/10.1016/j.scriptamat.2009.06.012>
12. Badge, S. K., Deshpande, A. V., "Effect of vanadium doping on structural, dielectric and ferroelectric properties of bismuth titanate ($\text{Bi}_4\text{Ti}_3\text{O}_{12}$) ceramics", *Ceramics International*, Vol. 45, (2019), 15307-15313. <https://doi.org/10.1016/j.ceramint.2019.05.021>
13. Chen, X. Q., Yang, F. J., Cao, W. Q., Wang, H., Yang, C. P., Wang, D. Y., Chen, K., "Enhanced multiferroic characteristics in Fe-doped $\text{Bi}_4\text{Ti}_3\text{O}_{12}$ ceramics," *Solid state communications*, Vol. 150, (2010),1221-1224. <https://doi.org/10.1016/j.ssc.2010.04.002>
14. Chen, Y., Pen, Z., Wang, Q., Zhu, J., "Crystalline structure, ferroelectric properties, and electrical conduction characteristics of W/Cr co-doped $\text{Bi}_4\text{Ti}_3\text{O}_{12}$ ceramics," *Journal of alloys and compounds*, Vol. 612, (2014),120-125. <https://doi.org/10.1016/j.jallcom.2014.05.136>
15. Lee, Y. C., Lee, T. K., Jan, J. H., "Piezoelectric properties and microstructures of ZnO-doped $\text{Bi}_{0.5}\text{Na}_{0.5}\text{TiO}_3$ ceramics", *Journal of the European ceramic society*, Vol. 31, (2011), 145-3152. <https://doi.org/10.1016/j.jeurceramsoc.2011.05.010>
16. Villegas, M., Jardiel, T., Caballero, A. C., "Effect of ZnO on the microstructure and electrical properties of $\text{WO}_3\text{-Bi}_4\text{Ti}_3\text{O}_{12}$ ceramics", *Journal of the European Ceramic Society*, Vol. 29, (2009), 737-742. <https://doi.org/10.1016/j.jeurceramsoc.2008.06.026>
17. Hayati, R., Bazargan-Lari, R., Zamani, A., Balak, Z., "Studying the effects of nano sintering additives on microstructure and electrical properties of potassium-sodium niobate piezoceramics," *Advanced Ceramics Progress*, Vol.4,(2018),7-15. [10.30501/ACP.2018.91120](https://doi.org/10.30501/ACP.2018.91120)
18. Slimani, Y., Selmi, A., Hannachi, E., Almessiere, M. A., Baykal, A., Ercan, I., "Impact of ZnO addition on structural, morphological, optical, dielectric and electrical performances of BaTiO_3 ceramics," *Journal of Materials Science: Materials in Electronics*, Vol. 30, (2019), 9520-9530. <https://doi.org/10.1007/s10854-019-01284-2>
19. Chou, C. S., Wu, C. Y., Yang, R. Y., Ho, C. Y., "Preparation and characterization of the bismuth sodium titanate ($\text{Na}_{0.5}\text{Bi}_{0.5}\text{TiO}_3$) ceramic doped with ZnO", *Advanced Powder Technology*, Vol. 23, (2012), 358-365. <https://doi.org/10.1016/j.apt.2011.04.015>
20. Rahaman, M. N., (2017), *Ceramic processing and sintering*. CRC press, <https://doi.org/10.1201/9781315274126>
21. Xie, S., Xu, J., Chen, Y., Jiang, L., Tan, Z., Nie, R., Xu, Q., Wang, Q. Zhu, J., "Poling effect and sintering temperature dependence on fracture strength and fatigue properties of bismuth titanate based piezoceramics", *Ceramics International*, Vol. 44, (2018), 20432-20440. <https://doi.org/10.1016/j.ceramint.2018.08.037>
22. Badge, S. K., & Deshpande, A. V. "Effect of pressure of pelletization on dielectric properties of Bismuth Titanate prepared by sol-gel synthesis", *Advanced Powder Technology*, Vol. 29, (2018), 555-562. <https://doi.org/10.1016/j.apt.2017.11.011>
23. Preethi, T. M., Ratheesh, R., "Synthesis and dielectric properties of a new class of $\text{MX}_6\text{Ti}_6\text{O}_{19}$ (M= Ba, Sr and Ca; X= Mg and Zn) ceramics", *Materials Letters*, Vol. 57, (2003), 2545-2552. [https://doi.org/10.1016/S0167-577X\(02\)01309-5](https://doi.org/10.1016/S0167-577X(02)01309-5)
24. Mesrar, M., Elbasset, A., Echadou, N. S., Abdi, F., Lamcharfi, T. D., "Studies of structural, dielectric, and impedance spectroscopy of KBT-modified sodium bismuth titanate lead-free ceramics", *ACS omega*, Vol. 7, (2022), 37142-37163. <https://doi.org/10.1021/acsomega.2c03139>